Proceedings of the 9th U.S. National and 10th Canadian Conference on Earthquake Engineering
Compte Rendu de la 9ième Conférence Nationale Américaine et
10ième Conférence Canadienne de Génie Parasismique
July 25-29, 2010, Toronto, Ontario, Canada • Paper No 348

SEISMIC BEHAVIOR OF A HYBRID PRECAST CONCRETE WALL SPECIMEN: MEASURED RESPONSE VERSUS DESIGN PREDICTIONS

B. J. Smith[1] and Y. C. Kurama[2]

ABSTRACT

This paper presents the results from the testing of a 0.4-scale "hybrid" precast concrete wall specimen under reversed-cyclic lateral loads combined with gravity loading. The specimen was designed to conform to the requirements of ACI ITG-5.2 (2009) and tested according to ACI ITG-5.1 (2007) to ultimately support the validation of hybrid precast walls for use in moderate and high seismic regions based on ACI 318 (2008). The measured behavior of the structure is discussed and compared with design predictions, focusing specifically on the applied lateral load and displacement, energy dissipation, performance of the steel reinforcement, and behavior along the horizontal base-panel-to-foundation and panel-to-panel joints. The test structure was not able to reach the maximum required drift level due to a combination of poor unconfined concrete strength and poor placement of the confinement reinforcement at the toes. However, the performance of the wall up to this premature failure level was consistent with the expected behavior, thus validating the procedure that was used in the design of the structure.

Introduction

As shown in Fig. 1, the hybrid precast concrete wall system investigated in this research utilizes a combination of mild (i.e., Grade 60) steel and high-strength unbonded post-tensioning (PT) steel for lateral resistance across horizontal joints. The PT steel is provided by multi-strand tendons placed inside un-grouted ducts to prevent bond between the steel and concrete. Thus, the tendons are connected to the structure only at end anchorages. Under the application of lateral loads into the nonlinear range, the primary mode of displacement in these walls occurs through gap opening at the horizontal joint between the base panel and the foundation. Upon unloading, the PT steel provides a restoring force to close this gap, thus reducing the residual (i.e., permanent) lateral displacements of the wall after a large earthquake. The use of unbonded PT tendons delays the yielding of the strands and reduces the tensile stresses transferred to the concrete (i.e., reduced cracking) as the tendons elongate under lateral loading. The mild steel bars crossing the horizontal joint at the base are designed to yield in tension and compression, and provide energy dissipation through the gap opening/closing behavior of the wall. A pre-determined length of these mild steel

[1]Graduate Student, Dept. of Civil Engineering, 156 Fitzpatrick Hall, Univ. of Notre Dame, Notre Dame, IN 46556
[2]Associate Professor, Dept. of Civil Engineering, 156 Fitzpatrick Hall, Univ. of Notre Dame, Notre Dame, IN 46556

bars is unbonded (by wrapping the bars with plastic sleeves) to prevent low-cycle fatigue fracture. Both the PT steel and mild steel contribute to the lateral strength of the wall, resulting in an efficient structure.

Hybrid precast concrete wall structures can offer high quality production, simpler construction, and excellent seismic characteristics. However, these walls are currently not allowed by ACI 318 (2008) unless their lateral performance is demonstrated through experimental evidence and analysis. To address this limitation, the primary objective of this ongoing research project at the University of Notre Dame is to experimentally and analytically validate hybrid wall structures for code approval according to the guidelines, prerequisites, and requirements in ACI ITG-5.1 (2007) and ACI 318. The specific project objectives are to develop: (1) a validated seismic design procedure for the hybrid precast wall system; (2) validated analytical models and design tools; and (3) practical guidelines and experimental evidence demonstrating the performance of these structures under lateral loading. In accordance with these objectives, the current paper compares the design predictions with the measured behavior of a wall specimen that was recently tested. The procedure that was used to design the test specimen and the results from a pre-test analytical study can be found in Smith and Kurama (2009).

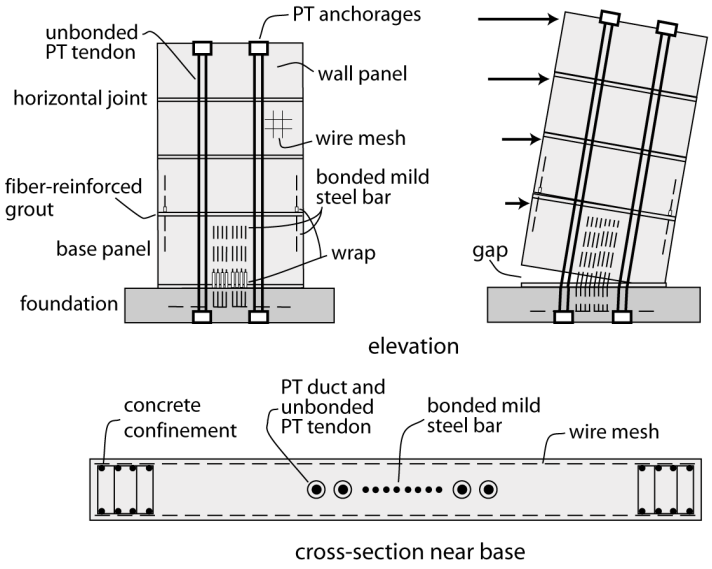

Figure 1. Elevation, Exaggerated Displaced Position, and Cross-Section of Hybrid Wall System

Validation and Testing Requirements

The roadmap to the code validation of hybrid precast concrete walls is provided by ACI ITG-5.1, which lays out the minimum experimental evidence needed for the classification of these walls as "special" reinforced concrete (RC) shear walls based on ACI 318. Specific requirements are given with regards to the tested wall roof drift, Δ_w, measured wall lateral strength to the predicted strength ratio, PT strand stresses and strains, amount of energy dissipation, wall strength degradation, and shear slip along the horizontal joints, among other requirements. The design is conducted at two levels of wall drift as follows: (1) the design-level drift, Δ_{wd}, which is determined according to the requirements of ASCE 7 (2006); and (2) the validation-level drift, which is defined by ACI ITG-5.1 as:

$$\Delta_{wm} = 0.9\% \le 0.8\left(h_w / l_w\right) + 0.5 \le 3.0\% \qquad (1)$$

where, h_w is the height to the top of the wall, and l_w is the length of the wall. The wall drift, Δ_w is defined as the lateral displacement at the top of the wall divided by the wall height. Prior to the validation testing, ACI ITG-5.1 requires that a pre-test design/analysis procedure for the specimen be established. A few key ACI ITG-5.1 requirements for each test specimen include: (1) a

minimum of two wall panels (in order to model a representative panel-to-panel joint as well as the base-panel-to-foundation joint) unless the prototype structure uses a single panel for the entire height of the wall; (2) a minimum specimen scale of one-third; (3) a minimum wall height-to-length aspect ratio of 0.5; and (4) the use of similar reinforcement details and representative building materials in the test specimen as in the full-scale prototype structure.

Prototype Wall Design

Specific guidelines for the design of special unbonded post-tensioned precast shear walls satisfying ACI ITG-5.1 are given in ACI ITG-5.2 (2009). Following these basic guidelines as well as those in ACI 318, a prototype structure was designed in collaboration with the Consulting Engineers Group (CEG), Texas. The prototype structure, shown in Fig. 2a, is a four-story regularly-shaped precast concrete parking garage with a footprint area of approximately 40,600-ft^2. The first story height is 12-ft while the upper story heights are 11-ft. The structure is located in Los Angeles, California, where the seismic response coefficient for the building was calculated as C_s=0.182g.

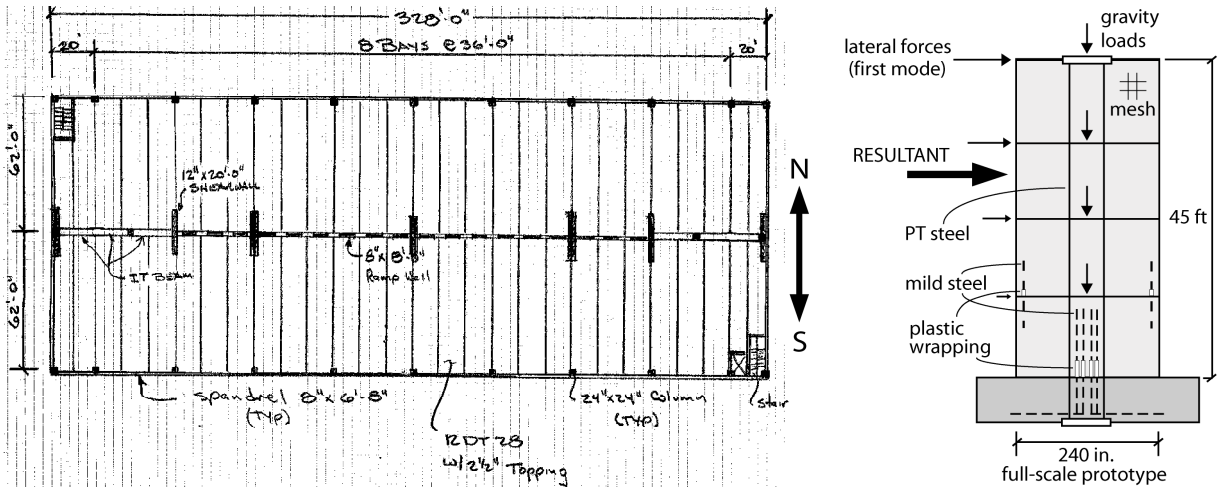

(A) (B)

Figure 2. Prototype Structure: (a) Plan View (Courtesy of CEG); (b) Wall Elevation

The lateral load resistance of the building in the N-S direction is provided by seven hybrid walls (see Fig. 2b for wall elevation). Using the equivalent lateral force procedure in ASCE 7 (2006), the design base moment demand for the exterior walls (where the lateral force demand is largest considering accidental torsion effects) can be determined as M_{wd}=20,000 kip-ft. A response modification factor of R=6.0 for special RC shear walls was used in the design. For the selected wall dimensions of h_w=45-ft and l_w=20-ft (resulting in an aspect ratio of 2.25), the validation-level drift from Eq. 1 is Δ_{wm}=2.30% and the design-level drift from ASCE 7 is Δ_{wd}=0.40%. In the calculation of Δ_{wd}, a displacement amplification factor of C_d=5.0 was applied to the linear-elastic displacement (flexural plus shear displacements) of the wall determined using an assumed cracked flexural stiffness of I_{cr}=0.60I_{gross} and a shear area of A_{sh}=0.67A_{gross}.

The specimen design procedure, described in more detail in Smith and Kurama (2009), provides specific steps to determine the PT and mild steel areas, the confined concrete detailing at

the wall ends, and the behavior at the horizontal joints both at the base and the upper floor levels (only the base joint is allowed to have significant gap opening). The energy dissipating mild steel reinforcement was designed to resist about 37% of the total base moment for the wall, with the remaining base moment demand resisted by the PT steel and the applied gravity load. According to ACI ITG-5.2, this design represents the approximate upper bound for the amount of mild steel that can be placed in the wall while maintaining the self-centering capability of the structure. It should be noted that the test specimen was intentionally designed not to have any significant over-strength beyond the minimum requirements of ACI ITG-5.2 and ACI 318. This decision was made in an effort to determine if the procedure and requirements used in the design of the wall were overly conservative, not conservative enough, or reasonable.

Test Set-Up and Specimen Properties

Fig. 3a shows a photograph of the test specimen and Fig. 3b shows a schematic of the test setup. The test was conducted at 0.4-scale, which satisfies the minimum scaling limit of ACI ITG-5.1. The lateral load was applied at the resultant location of the 1st mode inertial forces (12-ft from the wall base), resulting in a wall base moment to shear ratio of $M_b/V_b=1.5l_w$. A downward axial load of about 73 kips was applied at the centerline of the wall at the top to simulate the service-level gravity loads acting on the prototype structure. The test wall featured two panels: the base panel representing the 1st story and the upper panel representing the 2nd through 4th stories, thereby satisfying the ACI ITG-5.1 requirement for testing multi-panel walls. Note that it was possible to model the upper story panels of the prototype wall as a single panel since the joints between these panels were designed not to have any gap opening.

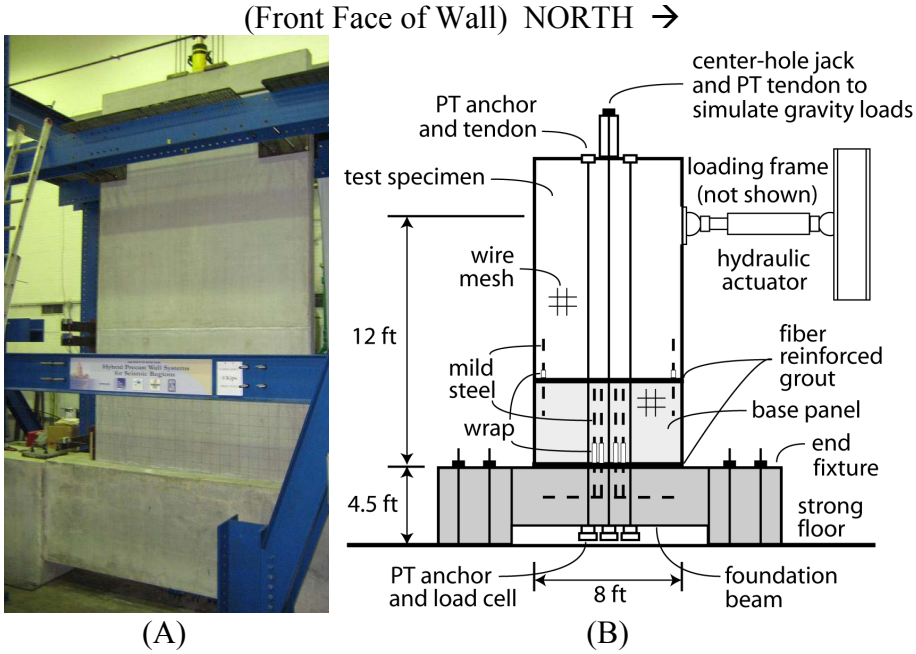

Figure 3. Test Set-Up: (a) Photograph; (b) Schematic Drawing

The 0.4-scale test wall length, l_w, was 96-in, the height of the base panel, h_{pb}, was 57.5-in, and the wall panel thickness, t_w, was 6.25-in. The PT steel consisted of two tendons located 9-in north and south from the wall centerline. Each tendon included three 0.5-in diameter strands (design ultimate strength, f_{pu}=270-ksi) with an unbonded length from the top of the wall to the bottom of the foundation beam of about 18-ft. The average initial stress in the tendons, calculated from the individual strand forces prior to the application of the lateral load, was $f_{pi}=0.55f_{pu}$. The mild steel (i.e., energy dissipating steel) crossing the base joint consisted of four No. 6 bars

(measured yield strength, f_{sy}=65-ksi), with one pair of bars placed 6-in north and south from the wall centerline and the other pair 3-in north and south from the centerline. The energy dissipating bars were unbonded over a length of 10-in at the bottom of the base panel. Across the panel-to-panel joint, only two No. 6 bars were used, with one bar located 4-in from each end of the wall. This reinforcement was not designed to yield or dissipate energy, but to control any gap opening along the panel-to-panel joint. To prevent strain concentrations in the panel-to-panel joint reinforcement, a short 3-in length of the bars was unbonded at the bottom of the upper panel. The design unconfined concrete strength for the wall was 6.0-ksi and the design confined concrete strength (within the toes of the base panel) was 9.0-ksi. However, the unconfined concrete strength for the base panel was only 4.8-ksi on the day that the wall was tested.

Measured Behavior of Specimen

As shown in Fig. 4a, a reversed-cyclic lateral displacement history was used during the test, with three fully-repeated cycles at each displacement increment. Fig. 4b depicts the measured base shear force, V_b versus wall drift, Δ_w behavior from the test and Fig. 4c shows a photograph of the lower half of the wall during the third cycle at Δ_w=+1.90% (note the gap opening at the north end). The wall drift, Δ_w, was measured as the relative lateral displacement of the wall between the lateral load location and the foundation divided by the height to the lateral load. The specimen sustained three cycles at a maximum positive drift (with the wall displaced southward) of Δ_w=+1.90% and a maximum negative drift of Δ_w=-1.55% prior to failure due to the crushing of the confined concrete at the toes. Fig. 4d shows the south toe of the wall at the end of the test. It can be seen that the first confinement hoop was placed at a significant angle with the horizontal, resulting in a large region of unconfined concrete at the bottom of the base panel (at the east face of the panel, the first hoop was located 4.5-in from the bottom rather than the design location of 2-in). While not as extreme as the south toe, the hoop placement at the north toe was also misaligned. This misalignment of the confinement hoops, combined with the low unconfined concrete strength (4.8-ksi rather than the design strength of 6.0-ksi) of the critical base panel, resulted in the premature failure of the wall at a lower drift level than expected.

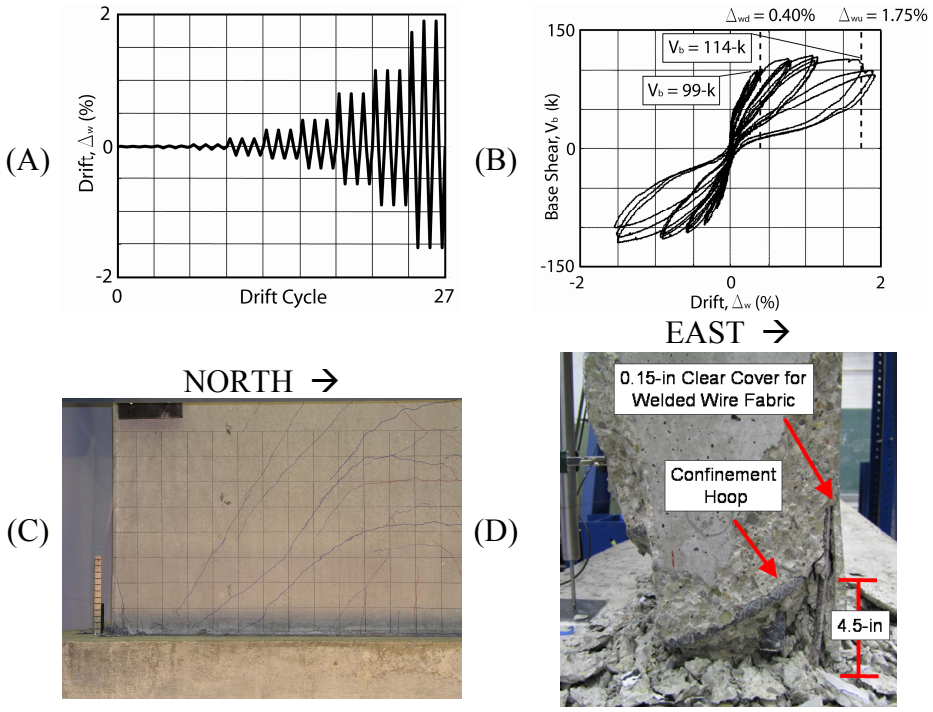

Figure 4. Wall Behavior: (a) Applied Displacement History; (b) V_b-Δ_w Response; (c) Damage at Third Cycle of Δ_w=+1.90%; (d) South Toe of Wall after Completion of Test

Fig. 5 shows the progression of damage at the south end of the wall under increasing drift as follows: (a) third cycle at Δ_w=+0.25%; (b) first cycle at Δ_w=+0.40; (c) third cycle at Δ_w=+1.15%; and (d) third cycle at Δ_w=+1.90%. The photographs highlight the initiation of cracking in the base panel, which occurred during the first cycle of Δ_w=+0.40% (Fig. 5b). Additionally, Figs. 5b through 5d show the progression of cracking and the initiation of cover concrete spalling at the south toe of the wall. Significant crushing of the wall concrete was not present until the final drift series of Δ_w=+1.90 (note that the extent of crushing at the south toe is more evident in Fig. 4d). The crushing of the confined concrete initiated at about Δ_w=+1.75%, after which the specimen started to undergo significant strength degradation as reflected by the V_b-Δ_w behavior during the second and third cycles at Δ_w=+1.90% in Fig. 4b. The test was stopped after the third cycle in this displacement series since the total strength degradation of the wall was approximately 20%, which is the strength degradation limit given by ACI ITG-5.1. Due to the smaller actual displacements reached, the performance of the wall in the negative drift direction was slightly better, with a smaller amount of strength degradation (~16%). No concrete cracking or spalling was observed in the upper panel throughout the test (see Fig. 4c).

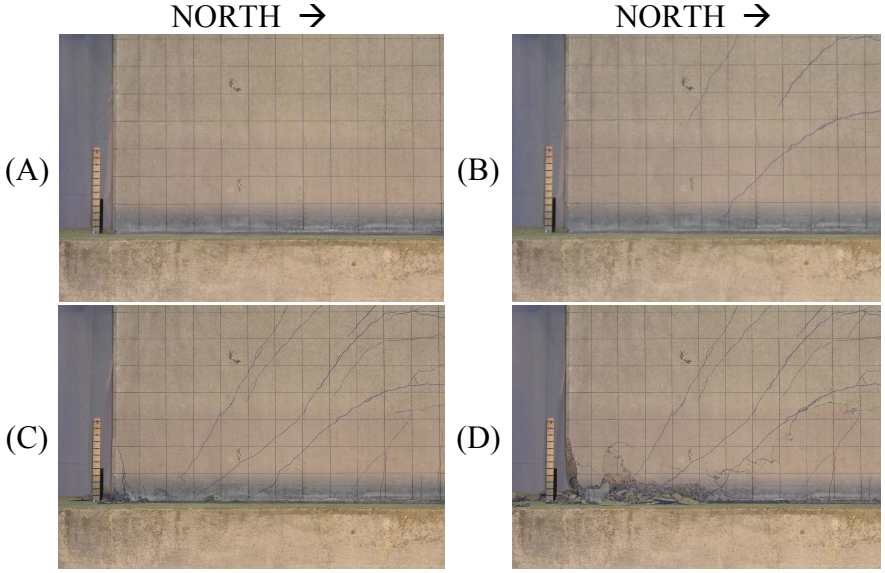

Figure 5. South End of Base Panel: (a) Δ_w=+0.25%-Third Cycle; (b) Δ_w=+0.40%-First Cycle; (c) Δ_w=+1.15%-Third Cycle; (d) Δ_w=+1.90%-Third Cycle

Comparisons between the predicted values for key material and behavioral aspects of the test structure (as determined using the design procedure in Smith and Kurama 2009) with the measured values are provided in Table 1. Note that instead of the validation-level wall drift, Δ_{wm}=2.30% (which was not achieved by the specimen), the comparisons are provided using the "failure-level" drift, Δ_{wu}=+1.75%. The failure-level drift was determined as the actual drift level reached when crushing of the confined concrete was observed and, for the subsequent larger drift cycles, significant strength degradation occurred in the V_b-Δ_w behavior.

Table 1. Comparisons of Predicted and Measured Results

Design Parameter	Design Drift, Δ_{wd}=+0.40%		Failure Drift, Δ_{wu}=+1.75%	
	Predicted	Measured	Predicted	Measured
Applied Lateral Load	98-kips	99-kips	118-kips	114-kips
Intermed. Mild Steel Strains	1.1 and 1.4%	0.6 and 1.2%	5.5 and 6.5%	---
Average PT Steel Stresses	0.58 and 0.62f_{pu}	0.58 and 0.63f_{pu}	0.73 and 0.84f_{pu}	0.70 and 0.82f_{pu}
Maximum Gap Opening	0.32-in	0.32-in	1.44-in	1.52-in
Neutral Axis Depth at Base	16.7-in	15.2-in	13.8-in	17.8-in

Applied Lateral Load

The maximum applied lateral load measured during the test was 120-kips, which was reached at Δ_w=+1.15%. The measured load at the design-level drift (Δ_{wd}=+0.40%) was 99-kips and at the failure-level drift (Δ_{wu}=+1.75%) was 114-kips. As shown in Table 1, these measurements compare very well with the predicted values at both drift levels.

Energy Dissipation

Energy dissipation in the hybrid wall system was achieved through the gap opening and closing behavior at the base-panel-to-foundation joint, which allowed for the reversed-cyclic yielding of the mild steel reinforcement over the unbonded length of the bars. To quantify the energy dissipation of the structure, ACI ITG-5.1 uses the energy dissipation ratio β, which is "the ratio of the measured energy dissipated by the test module during reversing cyclic displacements between given measured drift angles to the maximum theoretical energy that can be dissipated for the same drift angles." As defined and required in ACI ITG-5.1, β should be a minimum of 0.125 at the validation-level drift. Fig. 6 shows the measured energy dissipation of the test structure plotted against the wall drift. Note that the third cycle for each drift level was used to calculate the β ratios in this plot, except for the last series, where both the first and third cycles were used. It can be seen that the specimen exceeded the minimum energy dissipation requirement at drift levels greater than Δ_w=+0.80% and achieved a maximum β ratio of 0.20 at Δ_{wu}=+1.75%. The strength degradation at the end of the test resulted in a reduction in β.

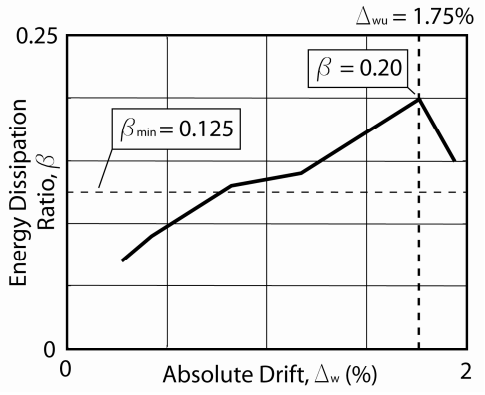

Figure 6. Energy Dissipation Ratio

Energy Dissipating Mild Steel Behavior

Since the mild steel reinforcement crossing the base joint serves as the main energy dissipater for the wall system, it is essential for the bars to yield before the design-level drift, but not fracture prior to the validation-level drift. Fig. 7a shows the four mild steel bars at the bottom of the base panel, prior to the placement of the concrete. The 10-in long plastic-wrapped unbonded length of the bars can be seen in the photograph, which was done to reduce the steel strains while the base-

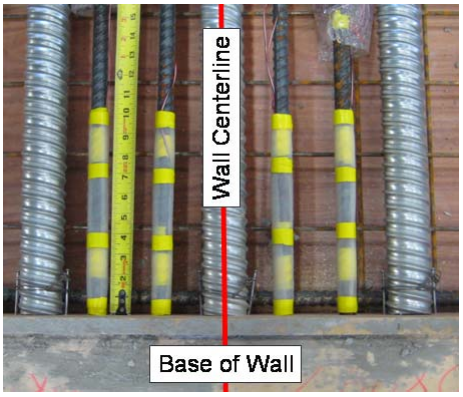

(A)

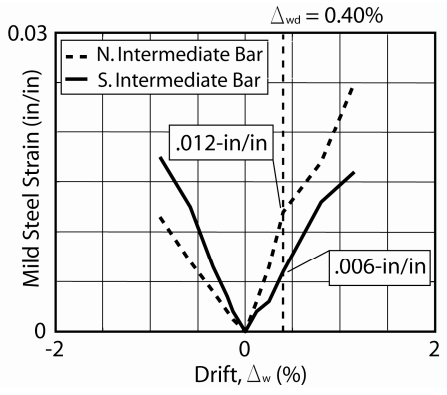

(B)

Figure 7. Mild Steel Reinforcement Crossing Base Joint: (a) Bar Placement; (b) Strains in North and South Intermediate Bars

panel-to-foundation joint was subjected to large gap opening. Furthermore, the bars were located near the centerline of the wall to reduce the strains and, in turn, reduce the required unbonded length. Fig. 7b shows the measured strains of the middle two bars (referred to as the north intermediate and south intermediate bars, located ±3-in from the wall centerline) using strain gauges placed within the unbonded length. As designed, the mild steel bars yielded (measured yield strain, ε_{sy}=0.00227-in/in) relatively early in the test and prior to the design-level drift, Δ_{wd}=0.40%. As shown in Table 1, the measured steel strains at Δ_{wd}=+0.40%, which were 0.006 and 0.012-in/in for the south and north bars, respectively, are reasonably close to the predicted strains of 0.011 and 0.014-in/in. The differences in the north and south mild steel stains are due to the different elongations of the two bars when the wall was displaced laterally. At the failure-level drift of Δ_{wu}=+1.75%, the predicted strains in the intermediate bars were 0.055 and 0.065-in/in; however, no measurements were made due to gauge failure.

PT Steel Behavior

The PT steel provides the main restoring force for the system, allowing the structure to return to its initial undisplaced position after being subjected to lateral loading. Fig. 8 depicts this restoring force, by plotting the normalized average stress in each of the north and south tendons (calculated as the sum of the measured strand forces divided by $A_p f_{pu}$, where A_p is the total area of the three 0.5-in diameter strands in each tendon and f_{pu}=270-ksi). Consistent with design expectations, the PT strands remained linear-elastic throughout the test, which was made possible since the strands were unbonded over their entire length. Note that relatively large losses in the PT steel stresses can be seen during the second and third cycles to Δ_w=+1.90% in Fig. 8. These losses occurred due to the crushing of the concrete at the wall base (which resulted in a small amount of axial "shortening" of the wall), and not due to nonlinear straining of the strands. Referring to Table 1, it can be seen that at both the design-level and failure-level drifts, the measured tendon stresses (0.58-0.63f_{pu} and 0.70-0.82f_{pu}, respectively) were nearly identical to the predicted stresses (0.58-0.62f_{pu} and 0.73-0.84f_{pu}, respectively). Similar to the mild steel reinforcement, the differences in the north and south tendon stresses are due to the different elongations of the two tendons as the wall was displaced laterally.

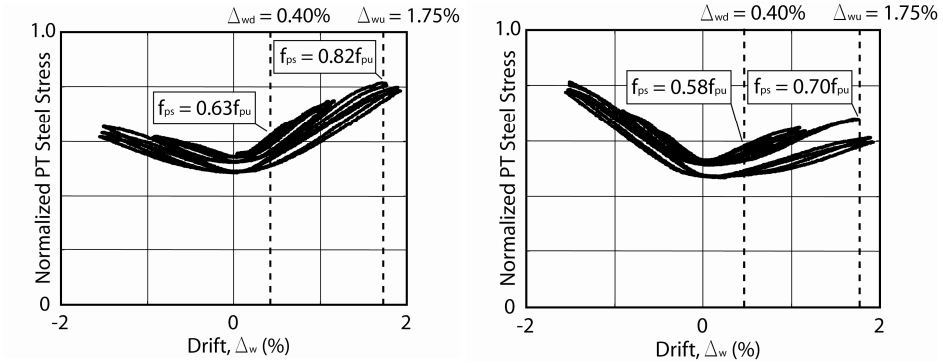

Figure 8. Average PT Steel Stresses: (a) North Tendon; (b) South Tendon

Gap Opening, Neutral Axis Depth, and Slip at Horizontal Joints

Consistent with the expected performance of the wall, the structure opened a significant gap at the base-panel-to-foundation joint. Fig. 9a shows the measured vertical size of this gap at the extreme north and south ends of the wall. In comparison, the gap opening at the panel-to-panel

joint was significantly smaller as designed (see Fig. 9b). At the failure drift of Δ_{wu}=+1.75%, the gap opening at the north end of the wall was approximately 1.52-in at the base joint (see Fig. 4c) and 0.06-in at the panel-to-panel joint. Referring to Table 1, the design procedure was able to successfully predict the size of the gap opening at the base joint.

Table 1 also compares the predicted and measured neutral axis depth (i.e., "contact" depth) at the base-panel-to-foundation joint of the wall. The neutral axis depth was measured using a combination of displacement and rotation transducers placed along the wall length at the base, as well as digital imaging techniques. The predicted neutral axis depths at the design drift (Δ_{wd}=+0.40%) and failure drift (Δ_{wu}=+1.75%) were 16.7-in and 13.8-in, respectively. The corresponding measured neutral axis depths were 15.2-in and 17.8-in, respectively. The relatively large discrepancy between the predicted and measured neutral axis depths at the failure drift could be related to the premature crushing of the concrete at the south end, which resulted in an increase in the neutral axis depth of the wall at the base.

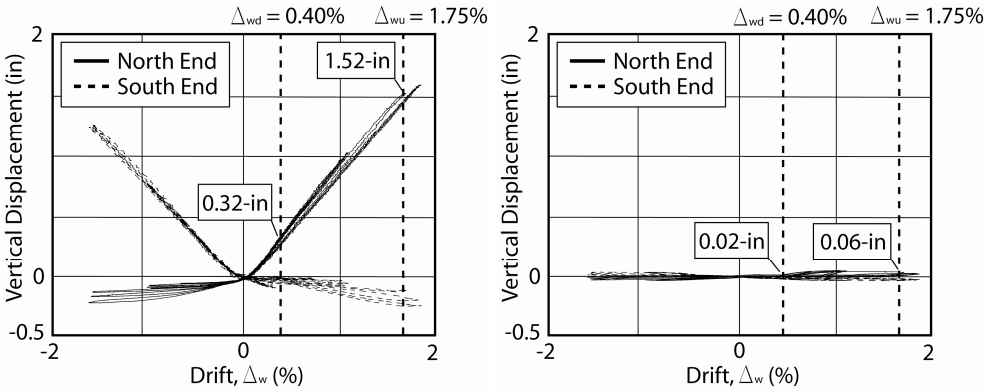

Figure 9. Vertical Gap Opening Displacement at Wall Ends:
(a) Base-Panel-to-Foundation Joint; (b) Panel-to-Panel Joint

The measured horizontal slip at the base-panel-to-foundation joint was extremely small, with the maximum measured slip less than 0.08-in. This amount of slip did not affect the performance of the wall in terms of strength degradation or any other undesirable behavior. The crushing of the concrete at the wall toes under increased drift demand did not appear to result in a disproportional increase in slip. No slip was observed at the upper panel-to-panel joint.

Recommendations

Relatively small changes to the detailing and construction of the wall are expected to improve the overall performance of the structure such that the validation-level drift, Δ_{wm} can be achieved in the future specimens to be tested as part of this project. First and foremost, appropriate attention will be paid to achieve the 6-ksi design compressive strength of the unconfined concrete, without significant over-strength on test day. Secondly, the first hoop reinforcement will be placed lower (at a height of approximately 0.75-in from the base) to ensure proper confinement of the concrete at the wall toes. Fabrication of the confinement cages will be done in a controlled laboratory environment to ensure proper placement and alignment of the hoops. Finally, while the design clear cover was 0.50-in for the welded wire fabric placed on each face of the wall panels, the actual clear cover was as little as 0.15-in near the south end of the base panel. As shown in Fig. 4d, this resulted in the delamination of the wire fabric near the end of the test. In future test specimens, the welded wire fabric will be replaced with evenly distributed horizontal and vertical

mild steel reinforcing bars at each wall face to ensure that an appropriate amount of concrete clear cover is achieved for this reinforcement.

Summary and Conclusions

This paper presents the results from an ongoing research project on the design and behavior of hybrid precast concrete wall structures for seismic regions. The measured lateral performance of a 0.4-scale test specimen is compared with the design predictions. Overall, the wall system performed as designed; however, failure occurred prematurely due to lower than specified unconfined concrete strength and poor placement of the confinement hoops at the wall toes. It is shown that the design procedure was able to result in a wall structure that achieved the required lateral strength, required energy dissipation, required performance of the mild steel and PT steel reinforcement, and required performance along the horizontal joints. Recommendations for relatively small changes to the detailing and construction of the walls to achieve the lateral displacement requirement are made based on the results.

Acknowledgments

This research is funded by the Charles Pankow Foundation and the Precast/Prestressed Concrete Institute (PCI). Additional technical and financial support is provided by the High Concrete Group, LLC, the Consulting Engineers Group, Inc., and the University of Notre Dame. The authors would like to acknowledge the support of the PCI Research and Development Committee as well as the members of the Project Advisory Panel, who include Walt Korkosz (chair) of the Consulting Engineers Group, Inc., Ken Baur of the High Concrete Group, LLC, Neil Hawkins of the University of Illinois at Urbana-Champaign, S.K. Ghosh of S.K. Ghosh Associates, Inc., and Dave Dieter of Mid-State Precast, LP. The authors would also like to thank Michael J. McGinnis from the University of Texas at Tyler for his assistance with data acquisition. Additional assistance and material donations were provided by Julian Albrigo of ERICO International Corporation, Jenny Bass of Essve Tech Inc., Randy Ernest of Prestress Supply Inc., Chris Lagaden of Ecco Manufacturing, Stan Landry of Enerpac Precision SURE-LOCK, Richard Lutz of Summit Engineered Products, Shane Whitacre of Dayton Superior Corporation, and Steve Yoshida of Sumiden Wire Products Corporation. Any opinions, findings, conclusions, and/or recommendations expressed in this paper are those of the authors and do not necessarily represent the views of the individuals or organizations acknowledged above.

References

ACI 318, 2008, *Building Code Requirements for Structural Concrete (ACI 318-08) and Commentary*, ACI Committee 318.

ACI ITG-5.1, 2007, *Acceptance Criteria for Special Unbonded Post-Tensioned Precast Structural Walls Based on Validation Testing and Commentary*, ACI Innovation Task Group 5.

ACI ITG-5.2, 2009, *Requirements for Design of a Special Unbonded Post-Tensioned Precast Shear Wall Satisfying ACI ITG-5.1 and Commentary*, ACI Innovation Task Group 5.

ASCE 7, 2006, *Minimum Design Loads for Buildings and Other Structures*, American Society of Civil Engineers.

Smith, B. and Kurama, Y., 2009, Design of Hybrid Precast Concrete Walls for Seismic Regions, *ASCE Structures Congress*, Austin, TX.